Submillimeter-wave spectrum of carbonyl sulfide: rare isotopic species

Submillimeter-wave spectrum of carbonyl sulfide: rare isotopic species

Kazuhiro Kubo, Takashi Furuya, and Shuji Saito

Research Center for Development of Far-Infrared Region, Fukui University, Fukui 910-8507, Japan

Abstract

Rotational spectra of four rare isotopic species of OCS were observed in the 110–690 GHz region with a source-modulated submillimeter-wave spectrometer. Spectral lines of $^{18}O^{13}CS$, $O^{13}C^{36}S$, $^{18}OC^{36}S$, and $^{18}O^{13}C^{34}S$ were measured in their natural abundances, 21.4, 1.51, 0.29, and 0.95 ppm, respectively. The rotational constants and centrifugal distortion constants were precisely determined from observed line frequencies by least squares methods. In order to facilitate sensitivity examination in the submillimeter-wave region, transition frequencies and peak absorption coefficients were calculated and tabulated for the spectral lines of the four species up to the 1000 GHz region.

Keywords: OCS; Rare isotopic species; Submillimeter-wave spectrum; Absorption coefficient

1. Introduction

Sensitivity is essential for high-resolution spectroscopic studies and high sensitivity and high resolution are inherent in microwave spectroscopy. Microwave spectrometers have been tested since their inception using rotational transitions of carbonyl sulfide, OCS, as it is a linear molecule with a medium sized rotational constant and it has isotopically substituted species with various natural abundances.

For the first time, in 1946, Dakin et al. [1] measured the $J = 2$–1 transition of OCS at 24 GHz and observed a splitting due to the Stark effect. One year later Hillger et al. [2] extended measurements to $J = 5$–4 at 60.8 GHz. Townes et al. [3] studied several isotopic species and determined the r_0 structure of OCS. In the 1950s the frequency region covered was further extended to over 100 GHz as frequency multipliers were introduced to microwave spectroscopy. Gordy and his collaborators developed efficient multipliers: 121.6 GHz for $J = 10$–9 in 1951 [4], 218.9 GHz for $J = 18$–17 in 1953 [5], 291.8 GHz for $J = 24$–23 in 1954 [6], and 510.5 GHz for $J = 42$–41 in 1956 [7].

The sensitivity of spectrometers was further improved such that isotopically substituted species with low natural abundances were then studied. Dubrulle et al. [8] investigated several singly and doubly substituted isotopic species up to 320 GHz with beam-absorption spectroscopy and improved their molecular constants. Burenin et al. [9] broadened the measurement ranges up to 510 GHz mainly for a few doubly substituted species with natural abundance of less than 0.05% using a BWO submillimeter-wave spectrometer with an acoustic detector.

In 1982 Kisiel and Millen [10] examined spectral line data of OCS and its isotopic species and tabulated their transition frequencies and peak absorption coefficients in the region up to 300 GHz. This study by Kisiel and Millen was further used to assess the sensitivity of microwave spectrometers [11]. To date, transition frequencies have not been reported for spectral lines of rare isotopic species above 300 GHz.

In the present study we measured spectral lines of several doubly and triply substituted isotopic species of OCS with very low natural abundances and tabulated their transition frequencies and peak absorption coefficients up to 1000 GHz.

2. Experimental

A source-modulated submillimeter-wave spectrometer reported previously [12] was used in combination with a 2 m free space absorption cell. The source radiation in the region of 110–690 GHz was supplied by a series of multipliers driven by millimeter-wave klystrons with a harmonic number of 2, 3, 4 or 6. Four rare isotopic species, $^{18}O^{13}CS$, $O^{13}C^{36}S$, $^{18}OC^{36}S$, and $^{18}O^{13}C^{34}S$ were studied in their natural abundances, 21.4, 1.51, 0.29, and 0.95 ppm, respectively. Spectral lines were measured in the region of 110–690 GHz. Three isotopic species, $^{18}O^{13}CS$, $O^{13}C^{36}S$, and $^{18}O^{13}C^{34}S$, were studied at room temperature and the isotopic species, $^{18}OC^{36}S$, of lowest abundance in the present study at a temperature of 140–150 K. The sample pressure in the cell was about 4.4 Pa.

Spectral line frequencies of $^{18}O^{13}CS$ and $^{18}O^{13}C^{34}S$ were predicted using rotational constants reported previously [13]. When several low J transitions were measured, the related observed frequencies were used to determine rotational constants and centrifugal distortion constants more precisely, which were then used to predict even higher J transitions. Twenty six spectral lines were measured for the $^{18}O^{13}CS$ species between 113 and 682 GHz and 17 lines for the $^{28}O^{13}C^{34}S$ species in the 166–366 GHz region, as listed in Tables 1 and 2, respectively.

Two isotopic species, $O^{13}C^{36}S$ and $^{18}OC^{36}S$, have not been studied to date. Prior to the start of the experiments we predicted the rotational constants of both species using differences between rotational constants of singly and doubly substituted species calculated from the r_s structure of OCS [14]. However, this method gives about one megahertz uncertainty to the rotational constant, which means a frequency range of larger than 100 MHz needed to be surveyed at high sensitivity. Spectral lines of $O^{13}C^{36}S$ and $^{18}OC^{36}S$ are very weak in intensity and thus, require the spectrometers used for their observations to be of very high sensitivity. However, the high sensitivity measurements are frequently affected by other lines and base line distortion. The first trial in the detection of a line of $O^{13}C^{36}S$ was unsuccessful in the relatively high sensitivity region of 300 GHz.

Recently Watson and his collaborators [15] presented an ingenious method, the $r_m^{(2)}$ model, to relate the zero-point and equilibrium moments of inertia of a molecule. In the model, the r_m coordinates are fitted to

Table 1
Observed and calculated transition frequencies of $^{18}O^{13}C^{32}S$ (in MHz)

$J' \leftarrow J$	ν_{obs}[a]	$\Delta\nu$[b]
2 ← 1	22764.24(20)[c]	0.010
10 ← 9	113816.815(07)	0.010
15 ← 14	170716.718(17)	−0.006
20 ← 19	227606.422(21)	−0.041
21 ← 20	238982.860(25)	−0.031
22 ← 21	250358.724(29)	−0.025
23 ← 22	261734.007(23)	−0.003
24 ← 23	273108.648(16)	0.002
25 ← 24	284482.574(35)	−0.056[d]
28 ← 27	318600.356(22)	−0.047
30 ← 29	341341.857(33)	0.027
31 ← 30	352711.339(21)	0.003
32 ← 31	364079.972(33)	−0.028
33 ← 32	375447.800(23)	0.005
37 ← 36	420909.808(26)	0.062[d]
40 ← 39	454995.773(28)	0.014
42 ← 41	477714.407(34)	0.024
44 ← 43	500428.460(46)	0.013
46 ← 45	523137.771(49)	0.038
47 ← 46	534490.528(41)	0.012
48 ← 47	545842.037(42)	0.013
51 ← 50	579888.627(42)	0.007
53 ← 52	602579.500(39)	0.026
55 ← 54	625264.599(57)	0.027
56 ← 55	636604.868(64)	−0.028
57 ← 56	647943.692(41)	−0.007
59 ← 58	670616.618(47)	−0.019
60 ← 59	681950.681(47)	−0.035

[a] Values in parentheses indicate uncertainties due to the variances of the measured frequency and the uncertainty of the frequency standard in units of the last significant digits.

[b] Residuals in least-squares fit. $\Delta\nu = \nu_{obs} - \nu_{cal}$.

[c] Maki and Johnson [13].

[d] Not included in the least-squares fit.

Table 2
Observed and calculated transition frequencies of $^{16}O^{13}C^{36}S$ (in MHz)

$J' \leftarrow J$	ν_{obs}[a]	$\Delta\nu$[b]
14 ← 13	161747.779(16)	−0.025
15 ← 14	173299.156(24)	0.000
16 ← 15	184850.072(32)	−0.009
17 ← 16	196400.548(23)	−0.004
21 ← 20	242597.303(19)	−0.010
22 ← 21	254145.057(18)	−0.022
23 ← 22	265692.214(19)	−0.007
24 ← 23	277238.746(21)	0.038
25 ← 24	288784.510(25)	−0.003
26 ← 25	300329.619(25)	0.013
27 ← 26	311873.950(30)	−0.010
28 ← 27	323417.537(21)	−0.009
30 ← 29	346502.326(23)	0.027
31 ← 30	358043.399(25)	−0.011
32 ← 31	369583.639(44)	0.000
33 ← 32	381122.981(27)	0.024
39 ← 38	450338.156(44)	−0.002
41 ← 40	473401.317(36)	−0.002
42 ← 41	484931.162(40)	−0.002
45 ← 44	519513.415(36)	−0.002
48 ← 47	554084.147(38)	−0.001
50 ← 49	577124.521(39)	−0.001
52 ← 51	600159.206(67)	−0.001
54 ← 53	623187.973(40)	−0.001
56 ← 55	646210.596(45)	0.000

[a] Values in parentheses indicate uncertainties due to the variances of the measured frequency and the uncertainty of the frequency standard in units of the last significant digits.

[b] Residuals in least-squares fit. $\Delta\nu = \nu_{obs} - \nu_{cal}$.

$$I_0^\alpha = I_m^\alpha + c_\alpha \left(I_m^\alpha\right)^{1/2} + d_\alpha \left(\frac{m_1 m_2 \cdots m_N}{M}\right)^{1/(2N-2)}, \qquad (1)$$

where $I_m^\alpha = I_{\text{rigid}}^\alpha(r_m)$ and I_0^α is the zero-point (ground state) moment of inertia for a molecule having N atoms and c_α and d_α are constants for each principal axis. The second term in Eq. (1) represents the contribution of the zero-point vibrations and the third the contribution due to det G^{-1}, i.e. the inverse of Wilson's G matrix for the molecule. Watson et al. [15] analyzed the observed moments of inertia for 12 isotopic species of OCS using least squares methods to give $r_m^{(2)}(\text{CO}) = 1.15648(2)$ Å, $r_m^{(2)}(\text{CS}) = 1.56107(3)$ Å, $c = 0.0504(4)u^{1/2}$ Å^2, and $d = -0.0657(8)u^{1/2}$ Å^2 with a standard deviation of the fit of $6.5 \times 10^{-5} u$ Å^2. We applied their result to predict the rotational constants of $O^{13}C^{36}S$ and $^{18}OC^{36}S$, which were calculated to be 5777.14 and 5430.17 MHz, respectively. The centrifugal distortion constants of both species were assumed to be equal to those of species having rotational constants of similar magnitude. The $J = 23$–22 transition of $O^{13}C^{36}S$, which was predicted to be 265690.6 ± 2.0 MHz, was found to lie at 265692.2 MHz.

Spectral lines of $^{18}OC^{36}S$ were similarly detected and assigned. Twenty five spectral lines were measured for the $O^{13}C^{36}S$ species in the 161–646 GHz range, and 17 lines for the $^{18}OC^{36}S$ species between 162–380 GHz, as listed in Tables 3 and 4, respectively. Fig. 1 shows an example of weak spectral lines, the $J = 50$–49 transition of $O^{13}C^{36}S$ at room temperature, observed at 577124.492 MHz. The observed line frequencies were analyzed by least-squares methods, where the $J = 2$–1 transitions for $^{18}O^{13}C^{34}S$ and $^{18}O^{13}C^{34}S$ measured previously [13] were also included in the fits. The rotational constants and centrifugal distortion constants determined by this study are shown in Table 5.

Table 3
Observed and calculated transition frequencies of $^{18}O^{12}C^{36}S$ (in MHz)

$J' \leftarrow J$	ν_{obs}[a]	$\Delta\nu$[b]
15 ← 14	162891.769(20)	0.002
16 ← 15	173749.142(28)	−0.030
17 ← 16	184606.170(19)	−0.011
18 ← 17	195462.757(32)	−0.012
19 ← 18	206318.914(25)	0.002
20 ← 19	217174.602(44)	0.017
21 ← 20	228029.781(17)	0.019
23 ← 22	249738.525(24)	−0.009
24 ← 23	260592.099(20)	0.022
25 ← 24	271445.029(21)	0.001
27 ← 26	293149.111(33)	0.064[c]
30 ← 29	325699.993(50)	−0.009
31 ← 30	336548.843(42)	−0.025
32 ← 31	347397.006(24)	0.039
33 ← 32	358244.279(37)	0.005
34 ← 33	369090.753(25)	−0.011
35 ← 34	379936.405(26)	−0.008

[a] Values in parentheses indicate uncertainties due to the variances of the measured frequency and the uncertainty of the frequency standard in units of the last significant digits.
[b] Residuals in least-squares fit. $\Delta\nu = \nu_{\text{obs}} - \nu_{\text{cal}}$.
[c] Not included in the least-squares fit.

Table 4
Observed and calculated transition frequencies of $^{18}O^{13}C^{34}S$ (in MHz)

$J' \leftarrow J$	ν_{obs}[a]	$\Delta\nu$[b]
2 ← 1	22179.426(80)[c]	−0.033
15 ← 14	166331.609(12)	−0.021
16 ← 15	177418.257(13)	−0.013
17 ← 16	188504.493(13)	−0.004
18 ← 17	199590.300(17)	0.015
19 ← 18	210675.607(14)	−0.001
21 ← 20	232844.760(18)	0.005
22 ← 21	243928.537(15)	0.009
23 ← 22	255011.742(18)	0.009
24 ← 23	266094.332(17)	−0.012
25 ← 24	277176.332(17)	−0.003
26 ← 25	288257.604(24)	−0.077[d]
28 ← 27	310418.367(29)	0.037
29 ← 28	321497.573(22)	−0.011
30 ← 29	332576.097(20)	0.009
31 ← 30	343653.813(24)	−0.004
32 ← 31	354730.741(27)	−0.005
33 ← 32	365806.834(22)	−0.014

[a] Values in parentheses indicate uncertainties due to the variances of the measured frequency and the uncertainty of the frequency standard in units of the last significant digits.
[b] Residuals in least-squares fit. $\Delta\nu = \nu_{\text{obs}} - \nu_{\text{cal}}$.
[c] Maki and Johnson [13].
[d] Not included in the least-squares fit.

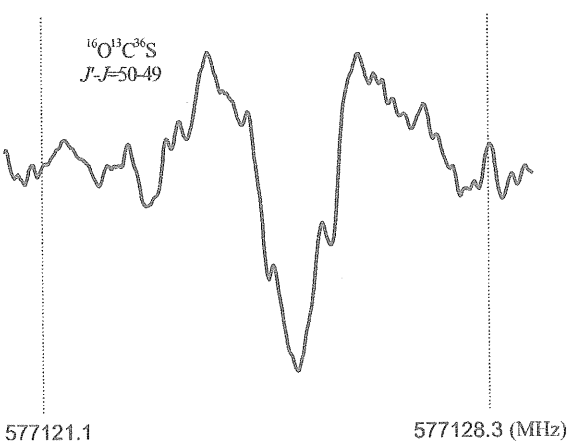

Fig. 1. A example of the observed spectral lines of $O^{13}C^{36}S$: $J = 50 \leftarrow 49$ transition. The gas pressure is 6.7 Pa and the temperature is 290 K The integration time was 80 s. The figure was recorded with upward scans in frequency.

3. Results and discussion

The molecular constants of the four rare isotopic species of OCS were precisely determined in the present

Table 5
Molecular constants for the four isotopic species of OCS (in MHz)[a]

	B_0	D_0	n_{fit} [b]	σ_{fit}
$^{18}O^{13}C^{32}S$	5691.06046(48)	0.00113108 7(93)	26	0.024
$^{16}O^{13}C^{36}S$	5777.17194(28)	0.00118534(67)	25	0.014
$^{18}O^{12}C^{36}S$	5430.18962(74)	0.00103126(42)	16	0.019
$^{18}O^{13}C^{34}S$	5544.87195(78)	0.00107620(47)	17	0.016

[a] Values in parentheses indicate three standard deviations in units of the last significant digits.
[b] Number of lines used in the fit.

Table 6
Calculated transition frequencies and peak absorption coefficients of $^{18}O^{13}C^{32}S$ in natural abundance at 296 K

$J' \leftarrow J$	ν_{calc} [a]	α_{max} [b]
1 ← 0	11382.128(0)	1.25×10^{-10}
2 ← 1	22764.24(20)[c]	1.02×10^{-9}
3 ← 2	34146.277(2)	3.52×10^{-9}
4 ← 3	45528.242(3)	8.44×10^{-9}
5 ← 4	56910.099(4)	1.62×10^{-8}
6 ← 5	68291.820(5)	2.74×10^{-8}
7 ← 6	79673.379(6)	4.25×10^{-8}
8 ← 7	91054.747(7)	6.19×10^{-8}
9 ← 8	102435.899(8)	8.59×10^{-8}
10 ← 9	113816.815(07)[d]	1.15×10^{-7}
11 ← 10	125197.441(10)	1.48×10^{-7}
12 ← 11	136577.779(11)	1.86×10^{-7}
13 ← 12	147957.790(12)	2.29×10^{-7}
14 ← 13	159337.449(13)	2.77×10^{-7}
15 ← 14	170716.718(17)[d]	3.28×10^{-7}
16 ← 15	182095.599(16)	3.83×10^{-7}
17 ← 16	193474.036(17)	4.42×10^{-7}
18 ← 17	204852.012(18)	5.03×10^{-7}
19 ← 18	216229.499(19)	5.66×10^{-7}
20 ← 19	227606.422(21)[d]	6.31×10^{-7}
21 ← 20	238982.860(25)[d]	6.97×10^{-7}
22 ← 21	250358.724(29)[d]	7.63×10^{-7}
23 ← 22	261734.007(23)[d]	8.29×10^{-7}
24 ← 23	273108.648(16)[d]	8.94×10^{-7}
25 ← 24	284482.574(35)[d]	9.58×10^{-7}
26 ← 25	295855.952(30)	1.02×10^{-6}
27 ← 26	307228.553(31)	1.08×10^{-6}
28 ← 27	318600.356(22)[d]	1.13×10^{-6}
29 ← 28	329971.532(35)	1.18×10^{-6}
30 ← 29	341341.857(33)[d]	1.23×10^{-6}
31 ← 30	352711.339(21)[d]	1.27×10^{-6}
32 ← 31	364079.972(33)[d]	1.31×10^{-6}
33 ← 32	375447.800(23)[d]	1.34×10^{-6}
34 ← 33	386814.729(44)	1.37×10^{-6}
35 ← 34	398180.709(47)	1.39×10^{-6}
36 ← 35	409545.738(49)	1.40×10^{-6}
37 ← 36	420909.808(26)[d]	1.41×10^{-6}
38 ← 37	432272.839(54)	1.42×10^{-6}
39 ← 38	443634.856(56)	1.42×10^{-6}
40 ← 39	454995.773(28)[d]	1.41×10^{-6}
41 ← 40	466355.688(61)	1.40×10^{-6}
42 ← 41	477714.407(34)[d]	1.38×10^{-6}
43 ← 42	489072.068(67)	1.36×10^{-6}
44 ← 43	500428.460(46)[d]	1.34×10^{-6}
45 ← 44	511783.781(73)	1.31×10^{-6}
46 ← 45	523137.771(49)[d]	1.27×10^{-6}
47 ← 46	534490.528(41)[d]	1.24×10^{-6}
48 ← 47	545842.037(42)[d]	1.20×10^{-6}
49 ← 48	557192.332(86)	1.16×10^{-6}
50 ← 49	568541.213(89)	1.11×10^{-6}

Table 6 (*continued*)

$J' \leftarrow J$	ν_{calc} [a]	α_{max} [b]
51 ← 50	579888.627(42)[d]	1.07×10^{-6}
52 ← 51	591234.876(97)	1.02×10^{-6}
53 ← 52	602579.500(39)[d]	9.77×10^{-7}
54 ← 53	613922.895(104)	9.30×10^{-7}
55 ← 54	625264.599(57)[d]	8.82×10^{-7}
56 ← 55	636604.868(64)[d]	8.35×10^{-7}
57 ← 56	647943.692(41)[d]	7.88×10^{-7}
58 ← 57	659281.127(121)	7.42×10^{-7}
59 ← 58	670616.618(47)[d]	6.96×10^{-7}
60 ← 59	681950.681(47)[d]	6.52×10^{-7}
61 ← 60	693283.367(136)	6.09×10^{-7}
62 ← 61	704614.172(141)	5.67×10^{-7}
63 ← 62	715943.295(146)	5.27×10^{-7}
64 ← 63	727270.707(151)	4.88×10^{-7}
65 ← 64	738596.383(156)	4.51×10^{-7}
66 ← 65	749920.294(162)	4.16×10^{-7}
67 ← 66	761242.414(168)	3.83×10^{-7}
68 ← 67	772562.716(173)	3.51×10^{-7}
69 ← 68	783881.172(179)	3.21×10^{-7}
70 ← 69	795197.756(185)	2.93×10^{-7}
71 ← 70	806512.439(192)	2.67×10^{-7}
72 ← 71	817825.196(198)	2.43×10^{-7}
73 ← 72	829136.00(20)	2.20×10^{-7}
74 ← 73	840444.820(21)	1.99×10^{-7}
75 ← 74	851751.63(22)	1.80×10^{-7}
76 ← 75	863056.41(23)	1.62×10^{-7}
77 ← 76	874359.12(23)	1.45×10^{-7}
78 ← 77	885659.75(24)	1.30×10^{-7}
79 ← 78	896958.26(25)	1.16×10^{-7}
80 ← 79	908254.62(26)	1.04×10^{-7}
81 ← 80	919548.81(26)	9.23×10^{-8}
82 ← 81	930840.81(27)	8.20×10^{-8}
83 ← 82	942130.57(28)	7.26×10^{-8}
84 ← 83	953418.09(29)	6.42×10^{-8}
85 ← 84	964703.33(30)	5.66×10^{-8}
86 ← 85	975986.25(31)	4.99×10^{-8}
87 ← 86	987266.85(32)	4.38×10^{-8}
88 ← 87	998545.08(32)	3.84×10^{-8}

[a] MHz. Calculated transition frequencies and estimated errors (3σ) in parentheses were obtained from molecular constants in Table 5.
[b] cm^{-1}, see text.
[c] Maki and Johnson [13].
[d] Present study.

study. The rotational constants and the centrifugal distortion constants of $O^{13}C^{36}S$ and $^{18}OC^{36}S$ were determined for the first time. Rotational constants of the two newly studied species are 5777.17194(28) MHz for $O^{13}C^{36}S$ and 5430.18962(74) MHz for $^{18}OC^{36}S$, and are compared with 5777.143 and 5430.174 MHz, respec-

Table 7
Calculated transition frequencies and peak absorption coefficients of $^{16}O^{13}C^{36}S$ in natural abundance at 296 K

$J' \leftarrow J$	ν_{calc}[a]	α_{max}[b]
1 ← 0	11554.339(0)	9.22×10^{-12}
2 ← 1	23108.650(1)	7.51×10^{-11}
3 ← 2	34662.904(1)	2.59×10^{-10}
4 ← 3	46217.072(2)	6.20×10^{-10}
5 ← 4	57771.127(2)	1.19×10^{-9}
6 ← 5	69325.039(3)	2.01×10^{-9}
7 ← 6	80878.781(3)	3.12×10^{-9}
8 ← 7	92432.323(4)	4.55×10^{-9}
9 ← 8	103985.638(5)	6.31×10^{-9}
10 ← 9	115538.697(5)	8.41×10^{-9}
11 ← 10	127091.472(6)	1.09×10^{-8}
12 ← 11	138643.933(6)	1.37×10^{-8}
13 ← 12	150196.054(7)	1.68×10^{-8}
14 ← 13	161747.779(16)[c]	2.03×10^{-8}
15 ← 14	173299.156(24)[c]	2.40×10^{-8}
16 ← 15	184850.072(32)[c]	2.81×10^{-8}
17 ← 16	196400.548(23)[c]	3.23×10^{-8}
18 ← 17	207950.538(11)	3.68×10^{-8}
19 ← 18	219500.013(11)	4.14×10^{-8}
20 ← 19	231048.947(12)	4.61×10^{-8}
21 ← 20	242597.303(19)[c]	5.09×10^{-8}
22 ← 21	254145.057(18)[c]	5.57×10^{-8}
23 ← 22	265692.214(19)[c]	6.05×10^{-8}
24 ← 23	277238.746(21)[c]	6.52×10^{-8}
25 ← 24	288784.510(25)[c]	6.98×10^{-8}
26 ← 25	300329.619(25)[c]	7.42×10^{-8}
27 ← 26	311873.950(30)[c]	7.83×10^{-8}
28 ← 27	323417.537(21)[c]	8.23×10^{-8}
29 ← 28	334960.335(21)	8.59×10^{-8}
30 ← 29	346502.326(23)[c]	8.92×10^{-8}
31 ← 30	358043.399(25)[c]	9.22×10^{-8}
32 ← 31	369583.639(44)[c]	9.48×10^{-8}
33 ← 32	381122.981(27)[c]	9.70×10^{-8}
34 ← 33	392661.337(27)	9.89×10^{-8}
35 ← 34	404198.749(29)	1.00×10^{-7}
36 ← 35	415735.166(30)	1.01×10^{-7}
37 ← 36	427270.559(32)	1.02×10^{-7}
38 ← 37	438804.899(33)	1.02×10^{-7}
39 ← 38	450338.156(44)[c]	1.02×10^{-7}
40 ← 39	461870.307(37)	1.01×10^{-7}
41 ← 40	473401.317(36)[c]	1.00×10^{-7}
42 ← 41	484931.162(40)[c]	9.90×10^{-8}
43 ← 42	496459.814(42)	9.74×10^{-8}
44 ← 43	507987.241(44)	9.55×10^{-8}
45 ← 44	519513.415(36)[c]	9.33×10^{-8}
46 ← 45	531038.312(48)	9.08×10^{-8}
47 ← 46	542561.899(50)	8.81×10^{-8}
48 ← 47	554084.147(38)[c]	8.53×10^{-8}
49 ← 48	565605.032(55)	8.22×10^{-8}
50 ← 49	577124.521(39)	7.91×10^{-8}
51 ← 50	588642.590(60)	7.58×10^{-8}
52 ← 51	600159.206(67)[c]	7.24×10^{-8}
53 ← 52	611674.344(65)	6.90×10^{-8}
54 ← 53	623187.973(40)	6.56×10^{-8}
55 ← 54	634700.067(70)	6.22×10^{-8}
56 ← 55	646210.596(45)	5.87×10^{-8}
57 ← 56	657719.532(76)	5.54×10^{-8}
58 ← 57	669226.846(79)	5.20×10^{-8}
59 ← 58	680732.510(82)	4.88×10^{-8}
60 ← 59	692236.496(85)	4.56×10^{-8}
61 ← 60	703738.775(89)	4.25×10^{-8}
62 ← 61	715239.318(92)	3.95×10^{-8}
63 ← 62	726738.098(96)	3.66×10^{-8}
64 ← 63	738235.086(99)	3.39×10^{-8}
65 ← 64	749730.252(103)	3.13×10^{-8}
66 ← 65	761223.570(107)	2.88×10^{-8}
67 ← 66	772715.010(111)	2.64×10^{-8}
68 ← 67	784204.544(115)	2.42×10^{-8}
69 ← 68	795692.144(119)	2.21×10^{-8}
70 ← 69	807177.781(123)	2.01×10^{-8}
71 ← 70	818661.426(128)	1.83×10^{-8}
72 ← 71	830143.051(132)	1.66×10^{-8}
73 ← 72	841622.628(137)	1.50×10^{-8}
74 ← 73	853100.129(141)	1.36×10^{-8}
75 ← 74	864575.524(146)	1.22×10^{-8}
76 ← 75	876048.786(151)	1.10×10^{-8}
77 ← 76	887519.885(156)	9.82×10^{-9}
78 ← 77	898988.795(161)	8.78×10^{-9}
79 ← 78	910455.485(167)	7.84×10^{-9}
80 ← 79	921919.927(172)	6.97×10^{-9}
81 ← 80	933382.094(178)	6.19×10^{-9}
82 ← 81	944841.957(183)	5.49×10^{-9}
83 ← 82	956299.487(189)	4.85×10^{-9}
84 ← 83	967754.655(195)	4.28×10^{-9}
85 ← 84	979207.43(20)	3.77×10^{-9}
86 ← 85	990657.80(21)	3.31×10^{-9}

[a] MHz. Calculated transition frequencies and estimated errors (3σ) in parentheses were obtained from molecular constants in Table 5.
[b] cm^{-1}, see text.
[c] Present study.

tively, predicted from Watson et al.'s $r_m^{(2)}$ model. The differences between observed and predicted values are surprisingly small, less than 30 kHz. This result ascertains that the model can be used for an exact prediction of the spectrum of isotopically substituted species with low abundances, as suggested by Watson et al. [15].

The transition frequencies of the four species and their estimated errors can be predicted up to 1000 GHz as shown in Tables 6–9. Other useful information to be added to each transition is the peak absorption coefficient, which was calculated by the method outlined by Kisiel and Millen [10]. The peak absorption coefficient α_{max} for a rotational transition of a linear molecule in the ground vibrational state is given by the following equation:

$$\alpha_{max} = 0.03930 \frac{aF_{GS}B^3\mu^2}{(T^2\Delta\nu^\theta)}(J+1)^3 \times \left(1 - \frac{0.02400\nu_0}{T}\right) e^{-0.02400J\nu_0/T}, \quad (2)$$

where a is the isotopic abundance for the molecular species involved, F_{GS} the fraction of involved molecules in the ground vibrational state, μ the electric dipole moment (D), T the temperature of the sample (K), ν_0 the transition frequency (GHz), and $\Delta\nu^\theta$ the standard half-width parameter (MHz) at standard temperature (300 K) and standard pressure (133 Pa). The units of α_{max} are cm^{-1} and B, GHz, and the expression for F_{GS} is given by

Table 8
Calculated transition frequencies and peak absorption coefficients of $^{18}O^{12}C^{36}S$ in natural abundance at 296 K

$J' \leftarrow J$	ν_{calc} [a]	α_{max} [b]
1 ← 0	10860.375(0)	1.44×10^{-12}
2 ← 1	21720.725(2)	1.17×10^{-11}
3 ← 2	32581.026(3)	4.03×10^{-11}
4 ← 3	43441.253(5)	9.68×10^{-11}
5 ← 4	54301.381(6)	1.86×10^{-10}
6 ← 5	65161.384(8)	3.14×10^{-10}
7 ← 6	76021.240(9)	4.88×10^{-10}
8 ← 7	86880.922(11)	7.11×10^{-10}
9 ← 8	97740.406(13)	9.88×10^{-10}
10 ← 9	108599.667(14)	1.32×10^{-9}
11 ← 10	119458.681(16)	1.71×10^{-9}
12 ← 11	130317.423(18)	2.15×10^{-9}
13 ← 12	141175.868(20)	2.65×10^{-9}
14 ← 13	152033.990(23)	3.20×10^{-9}
15 ← 14	162891.769(20)[c]	3.79×10^{-9}
16 ← 15	173749.142(28)[c]	4.44×10^{-9}
17 ← 16	184606.170(19)[c]	5.12×10^{-9}
18 ← 17	195462.757(32)[c]	5.84×10^{-9}
19 ← 18	206318.914(25)[c]	6.59×10^{-9}
20 ← 19	217174.602(44)[c]	7.35×10^{-9}
21 ← 20	228029.781(17)[c]	8.14×10^{-9}
22 ← 21	238884.420(45)	8.93×10^{-9}
23 ← 22	249738.525(24)[c]	9.72×10^{-9}
24 ← 23	260592.099(20)[c]	1.05×10^{-8}
25 ← 24	271445.029(21)[c]	1.13×10^{-8}
26 ← 25	282297.359(61)	1.20×10^{-8}
27 ← 26	293149.111(33)[c]	1.27×10^{-8}
28 ← 27	304000.066(70)	1.34×10^{-8}
29 ← 28	314850.393(75)	1.40×10^{-8}
30 ← 29	325699.993(50)[c]	1.46×10^{-8}
31 ← 30	336548.843(42)[c]	1.52×10^{-8}
32 ← 31	347397.006(24)[c]	1.57×10^{-8}
33 ← 32	358244.279(37)[c]	1.61×10^{-8}
34 ← 33	369090.753(25)[c]	1.65×10^{-8}
35 ← 34	379936.405(26)[c]	1.68×10^{-8}
36 ← 35	390781.196(119)	1.70×10^{-8}
37 ← 36	401625.087(126)	1.72×10^{-8}
38 ← 37	412468.063(134)	1.73×10^{-8}
39 ← 38	423310.098(142)	1.73×10^{-8}
40 ← 39	434151.168(151)	1.73×10^{-8}
41 ← 40	444991.248(160)	1.72×10^{-8}
42 ← 41	455830.313(169)	1.70×10^{-8}
43 ← 42	466668.339(179)	1.68×10^{-8}
44 ← 43	477505.300(189)	1.66×10^{-8}
45 ← 44	488341.173(199)	1.63×10^{-8}
46 ← 45	499175.93(21)	1.59×10^{-8}
47 ← 46	510009.55(22)	1.56×10^{-8}
48 ← 47	520842.01(23)	1.51×10^{-8}
49 ← 48	531673.28(25)	1.47×10^{-8}
50 ← 49	542503.33(26)	1.42×10^{-8}
51 ← 50	553332.15(27)	1.37×10^{-8}
52 ← 51	564159.71(29)	1.32×10^{-8}
53 ← 52	574985.98(30)	1.26×10^{-8}
54 ← 53	585810.94(31)	1.21×10^{-8}
55 ← 54	596634.56(33)	1.15×10^{-8}
56 ← 55	607456.82(35)	1.09×10^{-8}
57 ← 56	618277.69(36)	1.04×10^{-8}
58 ← 57	629097.15(38)	9.79×10^{-9}
59 ← 58	639915.18(40)	9.24×10^{-9}
60 ← 59	650731.75(41)	8.69×10^{-9}
61 ← 60	661546.83(43)	8.16×10^{-9}
62 ← 61	672360.40(45)	7.64×10^{-9}
63 ← 62	683172.44(47)	7.13×10^{-9}
64 ← 63	693982.92(49)	6.65×10^{-9}
65 ← 64	704791.82(51)	6.18×10^{-9}
66 ← 65	715599.10(53)	5.73×10^{-9}
67 ← 66	726404.75(55)	5.30×10^{-9}
68 ← 67	737208.75(58)	4.89×10^{-9}
69 ← 68	748011.06(60)	4.50×10^{-9}
70 ← 69	758811.66(63)	4.13×10^{-9}
71 ← 70	769610.53(65)	3.78×10^{-9}
72 ← 71	780407.65(68)	3.46×10^{-9}
73 ← 72	791202.99(70)	3.16×10^{-9}
74 ← 73	801996.50(73)	2.87×10^{-9}
75 ← 74	812788.20(75)	2.61×10^{-9}
76 ← 75	823578.03(78)	2.36×10^{-9}
77 ← 76	834365.99(81)	2.13×10^{-9}
78 ← 77	845152.04(84)	1.93×10^{-9}
79 ← 78	855936.16(87)	1.73×10^{-9}
80 ← 79	866718.32(90)	1.56×10^{-9}
81 ← 80	877498.51(94)	1.39×10^{-9}
82 ← 81	888276.69(97)	1.25×10^{-9}
83 ← 82	899052.84(100)	1.11×10^{-9}
84 ← 83	909826.94(104)	9.90×10^{-10}
85 ← 84	920598.95(107)	8.79×10^{-10}
86 ← 85	931368.87(111)	7.80×10^{-10}
87 ← 86	942136.65(114)	6.90×10^{-10}
88 ← 87	952902.28(118)	6.09×10^{-10}
89 ← 88	963665.73(122)	5.36×10^{-10}
90 ← 89	974426.99(126)	4.72×10^{-10}
91 ← 90	985186.01(130)	4.14×10^{-10}
92 ← 91	995942.78(134)	3.62×10^{-10}

[a] MHz. Calculated transition frequencies and estimated errors (3σ) in parentheses were obtained from molecular constants in Table 5.
[b] cm^{-1}, see text.
[c] Present study.

$$F_{GS} = \prod_i (1 - e^{-1.439\omega_i/T})^{di}.$$

A temperature of 296 K was used in the calculation. The dipole moment of the four isotopic species was assumed to be the same as that of the parent species, 0.71529 D [16]. Several methods including transient emission spectroscopy and absorption spectroscopy have been applied to measure the linewidths of rotational transitions of OCS. However, observed values of the standard half-width parameters are relatively random and their reliability has been discussed [17]. Cazzori and Dore [18] reported linewidth parameters of the $J = 8$–7, 12–11, and 16–15 transitions of $OC^{34}S$ by using absorption spectroscopy with frequency modulation. Since their result shows a clear J dependence, which agrees well with a theoretical prediction [19] and the difference between the linewidth parameters of different isotopic species is within 0.1 MHz/Torr, we can fit the three observed values for $OC^{34}S$ to the expression, $\Delta\nu^0(J) = 5.552 + 0.0613J$ by a least-squares method and readjust it to the most recent value for $J = 9$–8 of the parent species of OCS [20]: $\Delta\nu^0(J) = 5.428 + 0.0613J$. The linewidth parameter deviates from this

Table 9
Calculated transition frequencies and peak absorption coefficients of $^{18}O^{13}C^{34}S$ in natural abundance at 296 K

$J' \leftarrow J$	ν_{calc}[a]	α_{max}[b]
1 ← 0	11089.740(0)	5.00×10^{-12}
2 ← 1	22179.428(80)[c]	4.21×10^{-11}
3 ← 2	33269.115(3)	1.45×10^{-10}
4 ← 3	44358.700(5)	3.47×10^{-10}
5 ← 4	55448.181(6)	6.66×10^{-10}
6 ← 5	66537.534(8)	1.13×10^{-9}
7 ← 6	77626.731(10)	1.75×10^{-9}
8 ← 7	88715.747(12)	2.55×10^{-9}
9 ← 8	99804.557(13)	3.54×10^{-9}
10 ← 9	110893.134(15)	4.72×10^{-9}
11 ← 10	121981.453(18)	6.11×10^{-9}
12 ← 11	133069.488(20)	7.69×10^{-9}
13 ← 12	144157.213(22)	9.47×10^{-9}
14 ← 13	155244.602(24)	1.14×10^{-8}
15 ← 14	166331.609(12)[d]	1.36×10^{-8}
16 ← 15	177418.257(13)[d]	1.59×10^{-8}
17 ← 16	188504.493(13)[d]	1.83×10^{-8}
18 ← 17	199590.300(17)[d]	2.08×10^{-8}
19 ← 18	210675.607(14)[d]	2.35×10^{-8}
20 ← 19	221760.440(42)	2.62×10^{-8}
21 ← 20	232844.760(18)[d]	2.90×10^{-8}
22 ← 21	243928.537(15)[d]	3.18×10^{-8}
23 ← 22	255011.742(18)[d]	3.45×10^{-8}
24 ← 23	266094.332(17)[d]	3.73×10^{-8}
25 ← 24	277176.335(17)[d]	4.00×10^{-8}
26 ← 25	288257.604(24)[d]	4.26×10^{-8}
27 ← 26	299338.354(73)	4.51×10^{-8}
28 ← 27	310418.367(29)[d]	4.74×10^{-8}
29 ← 28	321497.573(22)[d]	4.96×10^{-8}
30 ← 29	332576.097(20)[d]	5.17×10^{-8}
31 ← 30	343653.813(24)[d]	5.35×10^{-8}
32 ← 31	354730.741(27)[d]	5.51×10^{-8}
33 ← 32	365806.834(22)[d]	5.66×10^{-8}
34 ← 33	376882.097(118)	5.78×10^{-8}
35 ← 34	387956.469(126)	5.88×10^{-8}
36 ← 35	399029.936(134)	5.95×10^{-8}
37 ← 36	410102.474(143)	6.00×10^{-8}
38 ← 37	421174.056(152)	6.03×10^{-8}
39 ← 38	432244.656(161)	6.04×10^{-8}
40 ← 39	443314.250(171)	6.02×10^{-8}
41 ← 40	454382.810(181)	5.98×10^{-8}
42 ← 41	465450.311(192)	5.92×10^{-8}
43 ← 42	476516.73(20)	5.84×10^{-8}
44 ← 43	487582.03(22)	5.74×10^{-8}
45 ← 44	498646.20(23)	5.63×10^{-8}
46 ← 45	509709.21(24)	5.50×10^{-8}
47 ← 46	520771.03(25)	5.36×10^{-8}
48 ← 47	531831.63(27)	5.20×10^{-8}
49 ← 48	542891.00(28)	5.04×10^{-8}
50 ← 49	553949.10(30)	4.86×10^{-8}
51 ← 50	565005.90(31)	4.68×10^{-8}
52 ← 51	576061.40(33)	4.49×10^{-8}
53 ← 52	587115.54(34)	4.29×10^{-8}
54 ← 53	598168.32(36)	4.10×10^{-8}
55 ← 54	609219.71(38)	3.90×10^{-8}
56 ← 55	620269.67(40)	3.70×10^{-8}
57 ← 56	631318.19(42)	3.50×10^{-8}
58 ← 57	642365.23(44)	3.30×10^{-8}
59 ← 58	653410.78(46)	3.11×10^{-8}
60 ← 59	664454.80(48)	2.92×10^{-8}
61 ← 60	675497.27(50)	2.73×10^{-8}
62 ← 61	686538.17(52)	2.55×10^{-8}
63 ← 62	697577.47(54)	2.38×10^{-8}
64 ← 63	708615.14(57)	2.21×10^{-8}
65 ← 64	719651.15(59)	2.05×10^{-8}
66 ← 65	730685.49(62)	1.90×10^{-8}
67 ← 66	741718.12(64)	1.75×10^{-8}
68 ← 67	752749.02(67)	1.61×10^{-8}
69 ← 68	763778.17(70)	1.48×10^{-8}
70 ← 69	774805.53(73)	1.35×10^{-8}
71 ← 70	785831.09(75)	1.24×10^{-8}
72 ← 71	796854.81(78)	1.13×10^{-8}
73 ← 72	807876.67(82)	1.03×10^{-8}
74 ← 73	818896.65(85)	9.31×10^{-9}
75 ← 74	829914.71(88)	8.43×10^{-9}
76 ← 75	840930.84(91)	7.62×10^{-9}
77 ← 76	851945.00(95)	6.86×10^{-9}
78 ← 77	862957.18(98)	6.17×10^{-9}
79 ← 78	873967.34(102)	5.54×10^{-9}
80 ← 79	884975.46(105)	4.96×10^{-9}
81 ← 80	895981.52(109)	4.43×10^{-9}
82 ← 81	906985.48(113)	3.95×10^{-9}
83 ← 82	917987.32(117)	3.51×10^{-9}
84 ← 83	928987.02(121)	3.12×10^{-9}
85 ← 84	939984.55(125)	2.76×10^{-9}
86 ← 85	950979.89(129)	2.44×10^{-9}
87 ← 86	961973.00(133)	2.15×10^{-9}
88 ← 87	972963.87(138)	1.89×10^{-9}
89 ← 88	983952.47(142)	1.66×10^{-9}
90 ← 89	994938.76(147)	1.46×10^{-9}

[a] MHz. Calculated transition frequencies and estimated errors (3σ) in parentheses were obtained from molecular constants in Table 5.
[b] cm^{-1}, see text.
[c] Maki and Johnson [13].
[d] Present study.

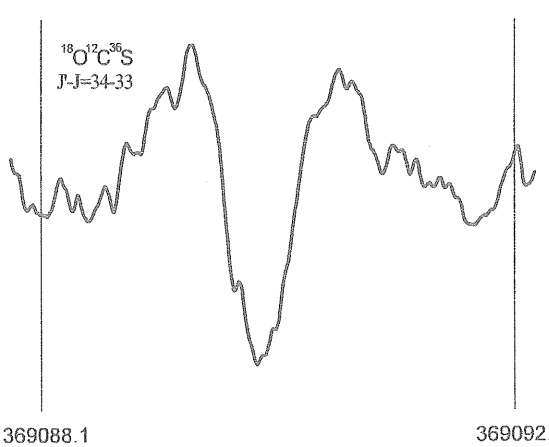

Fig. 2. The observed $J = 34 \leftarrow 33$ transition of the $^{18}O^{12}C^{36}S$ at a pressure of 6.7 Pa and a temperature of 290 K. The integration time was 160 s. The figure was recorded with upward scans in frequency.

expression at low J, because the linewidth of the lowest few transitions suffers from Dicke effect. Therefore, the values 6.05 [21], 5.92 [22], and 5.78 [23] MHz/Torr, which agree with other observed values and were determined by absorption spectroscopy, were used for the

$J = 1$–0, 2–1, and 3–2 transitions, respectively. The harmonic vibrational frequencies used in the calculation are 874.27 cm^{-1} for ω_1, 524.20 cm^{-1} for ω_2, and 2094.15 cm^{-1} for ω_3 [24]. The calculated peak absorption coefficients were also listed in Tables 6–9 for each transition. Calculated transition frequencies of OCS with their estimated errors and peak absorption coefficients are useful in examining submillimeter-wave spectrometers.

Fig. 2 shows an example of a rotational transition for the least abundant isotopic species, $^{18}O^{12}C^{36}S$: $J = 34$–33 at 369091 MHz at 290 K. The observed S/N ratio of 7–8 concludes that the sensitivity of our spectrometer given by a minimum detectable absorption coefficient is 4×10^{-9} cm^{-1} with a S/N ratio of 2.

Acknowledgments

The authors thank M.Takano for his help in measuring several spectral lines and I.K. Ahmad for her critical reading of the manuscript. The present study was supported by Grants-in-Aid from the Ministry of Education, Science, and Culture (No. 12440161).

References

[1] T.W. Dakin, W.E. Good, D.K. Coles, Phys. Rev. 70 (1946) 560.
[2] T.R.E. Hillger, M.W.P. Strandberg, T. Wentink Jr., R.L. Kyhl, Phys. Rev. 72 (1947) 157.
[3] C.H. Townes, A.N. Holden, F.R. Merrit, Phys. Rev. 74 (1948) 1113.
[4] C.M. Johnson, R. Trambarulo, W. Gordy, Phys. Rev. 84 (1951) 1178–1180.
[5] W. King, W. Gordy, Phys. Rev. 90 (1953) 319–320.
[6] W. King, W. Gordy, Phys. Rev. 93 (1954) 407–412.
[7] M. Cowan, W. Gordy, Phys. Rev. 104 (1956) 551–552.
[8] A. Dubrulle, J. Demaison, J. Burie, D. Boucher, Z. Naturforsch. 35a (1980) 471–474.
[9] A.V. Burenin, E.N. Karyakin, A.F. Krupnov, S.M. Shapin, A.N. Val'dov, J. Mol. Spectrosc. 85 (1981) 1–7.
[10] Z. Kisiel, D.J. Millen, J. Phys. Chem. Ref. Data 11 (1982) 101–117.
[11] S. Saito, Astron. Soc. Pacif. Conf. Ser. 16 (1991) 349–361.
[12] S. Saito, M. Goto, Astrophys. J. 410 (1993) L53–L55.
[13] A.G. Maki, D.R. Johnson, J. Mol. Spectrosc. 47 (1973) 226–233.
[14] C.C. Costain, J. Chem. Phys. 29 (1958) 864–874.
[15] J.K.G. Watson, A. Roytburg, W. Ulrich, J. Mol. Spectrosc. 196 (1999) 102–119.
[16] J.M.L. Reinartz, A. Dymanus, Chem. Phys. Lett. 24 (1974) 346–351.
[17] J. Doose, H. Mäder, R. Schwarz, A. Guarnieri, Mol. Phys. 3 (1994) 547–556.
[18] G. Cazzoli, L. Dore, J. Mol. Spectrosc. 141 (1990) 49–58.
[19] S.C. Mehrotra, J.E. Boggs, J. Chem. Phys. 66 (1977) 5306–5312.
[20] C. Puzzarini, L. Dore, G. Cazzoli, J. Mol. Spectrosc. 216 (2002) 428–436.
[21] C.O. Britt, J.E. Boggs, J. Chem. Phys. 45 (1966) 3877.
[22] S.C.M. Luijendik, J. Phys. B 10 (1977) 1741–1747.
[23] J.P.M. de Vreede, M.P.W. Gillis, H.A. Dijkerman, J. Mol. Spectrosc. 128 (1988) 509–520.
[24] Y. Morino, T. Nakagawa, J. Mol. Spectrosc. 26 (1968) 496–523.